UNIFIED THEORY OF PARTICLE-PHONON COUPLING: Application to Sb and In isotopes using a realistic interaction

HOONG-CHIEN LEE

Atomic Energy of Canada Limited, Chalk River Nuclear Laboratories, Chalk River, Ontario,

KOJ 1JO Canada

Received 14 September 1976 (Revised 11 March 1977)

Abstract: A self-consistent, unified, microscopic theory of particle-phonon coupling is applied to the Sb and In isotopes, which are treated as proton-particle and proton-hole states respectively coupled to the ground and low-lying vibrational states of Sn. The particle-phonon coupling interaction is derived from the same realistic two-body interaction which gives rise to the vibrational excitations in Sn. Spectroscopic factors, level schemes and B(E2) values calculated with no adjustable parameters are shown to be in good agreement with experimental data.

1. Introduction

The coupling of single-particle and collective degrees of freedom has long been known to exist in the nucleus. Specifically, the coupling of single-particle to nuclear vibrations, or phonons, is a well-known phenomenon. Foldy and Milford ¹) pointed out the effect of this coupling on the magnetic moments of odd-mass nuclei. Bohr and Mottelson ²) made a comprehensive study of the coupling in the liquid-drop model. More recently Castel *et al.* ³) studied this phenomenon in the 2s-1d shell, and Hamamoto ⁴) did an extensive study of this phenomenon in the Pb region. For the nuclei that will be studied in this work, the Sb isotopes have been investigated by Vanden Berghe and Heyde ⁵) and ¹¹⁵In by Dietrich *et al.* ⁶).

In the microscopic description of nuclear phenomena the surface vibration is described as coherent excitations of hole-particle pairs interacting through the residual nuclear two-body interaction ⁷). The same interaction should also provide a coupling between the single-particle and the vibrational motions. However, such a unified, or self-consistent treatment of the particle-phonon coupling has not so far been attempted. Compared to the simple phenomenological treatment ³⁻⁶) a self-consistent calculation is many-fold more complicated. For example, as a prerequisite the structure of the vibration must be calculated. In many cases such a calculation is quite lengthy. On the other hand, in a phenomenological calculation no knowledge of the vibration more than its excitation energy and multipolarity, which is obtained experimentally, need be known. Furthermore, such simple calculations have in most cases been reasonably successful. It is therefore not surprising that a unified treatment has been avoided.

In this paper we investigate the unified treatment of particle-phonon coupling. We show that a unified theory of particle-vibration coupling works very well indeed, at least in the Sn region. Here Sb is considered to be a proton-particle state coupled to the ground state and vibrations of Sn, and In is considered to be a proton-hole state coupled to Sn. We show that even though there is quite good agreement between theory and empirical data when no parameters are adjusted in the unified calculation, significantly better agreement is achieved when one or two collective properties of Sn are altered in the composite system in a reasonable manner.

In sect. 2 the formalism for the unified theory particle-phonon coupling is given. In sects. 3 and 4 results for the Sb isotopes and for ¹¹⁵In, respectively, are discussed and compared with experimental data. These results are obtained using a realistic interaction which had previously been shown to account for the important properties of the low vibrational states in the even Sn isotopes. Sect. 5 is a summary.

2. Formalism

For a system of interacting quasiparticles (qp) and phonons, the Hamiltonian with a two-body interaction can be written as

$$H = H_0 + \sum_{\alpha} E_{\alpha} a_{\alpha}^{\dagger} a_{\alpha} + \sum_{i} \omega_{i} Q_{\lambda}^{\dagger} Q_{\lambda} + \sum_{r \neq i} D_{r \neq \lambda} (Q_{\lambda}^{\dagger} a_{\delta}^{\dagger} a_{\gamma} + \text{h.c.}), \tag{1}$$

where a_{α}^{\dagger} (a_{α}) is a qp creation (annihilation) operator; Q_{λ}^{\dagger} is a phonon creation operator, H_0 is a constant; E_a is the qp energy; ω_l is the excitation energy of the phonon, and $D_{\gamma\delta\lambda}$ is particle-phonon coupling matrix element. The subscript a stands for all the quantum numbers of a single-particle (s.p.) orbital except the magnetic quantum number m_a , the Greek subscript $\alpha \equiv (a, m_a)$, and $\bar{\alpha} \equiv (a, -m_a)$; l is the angular momentum of the phonon, $\lambda \equiv (l, m_l)$ and $\bar{\lambda} = (l, -m_l)$. The qp operators are related to the s.p. operators $(c_{\alpha}^{\dagger}$ and c_{α}) by the Bogoljubov-Valatin ⁸) transformation,

$$a_a^{\dagger} = u_a c_a^{\dagger} - s_a v_a c_{\bar{a}}, \tag{2}$$

where $s_a = (-)^{j_a - m_a}$ and u and v are the qp occupational amplitudes satisfying $u_a^2 + v_a^2 = 1$. The phonon operators can be expressed in terms of qp operators ⁹)

$$Q_{\lambda}^{\dagger} = \sum_{a \geq b} \frac{1}{\sqrt{1 + \delta_{ab}}} (x_{ab}^{l} (A_{ab}^{\lambda})^{\dagger} - (-)^{l-aa} y_{ab}^{l} A_{ab}^{\lambda}), \tag{3}$$

$$(A_{\alpha\beta}^{\lambda})^{\dagger} = \sum_{\alpha, \beta, \alpha} C_{\alpha\beta}^{\lambda} a_{\alpha}^{\dagger} a_{\beta}^{\dagger}, \tag{4}$$

where $C_{a\beta}^{\lambda} \equiv \langle am_a bm_b | lm_i \rangle$ is a Clebsch-Gordan coefficient. The amplitudes x and y satisfy the orthonormal conditions:

$$\sum_{i} (x_{i}^{l} x_{i}^{l'} - y_{i}^{l} y_{i}^{l'}) = \delta_{ll'}, \tag{5}$$

$$\sum_{\sigma} \left(x_i^{l_{\sigma}} x_j^{l_{\sigma}} - y_i^{l_{\sigma}} y_j^{l_{\sigma}} \right) = \delta_{ij}, \tag{6}$$

where σ labels all phonons with the same l; i, j represent pairs of qp subscripts and in (5) only ordered qp $(a_i \ge b_i)$ pairs are summed over. The A, x and y all have the symmetry property

 $x_{ab}^{l} = -(-)^{j_a+j_b+l}x_{ba}^{l}. (7)$

The last term in (1) provides the coupling between quasiparticles and phonons. It can be derived from the same residual interaction that gives rise to the interaction between phonons. If the two-body residual interaction is $\frac{1}{4}V_{\alpha\beta\gamma\delta}C_{\alpha}^{\dagger}C_{\beta}C_{\delta}C_{\gamma}$, then the reduced particle-phonon interaction matrix element, $D_{cdl} \equiv D_{\gamma\delta\lambda}/C_{\delta\lambda}^{\dagger}$ is given by

$$D_{cdl} = \frac{1}{2} \sum_{ab} \sqrt{1 + \delta_{ab}} \sqrt{\frac{2l+1}{2j_c+1}} \left(F_{abcdl} u_c u_d + (-)^{j_c + j_d + l} F_{abcdl} v_c v_d \right) \times (x_{ab}^l u_a v_b + y_{ab}^l v_a u_b), \tag{8}$$

where the F-matrix elements are defined by

$$V_{e\beta\gamma\delta} = \sum_{i} C_{e\gamma}^{\lambda} S_{\gamma} C_{\delta\bar{\beta}}^{\lambda} S_{\beta} F_{ecdbl}. \tag{9}$$

The creation operator b_{γ}^{\dagger} for a particle-phonon coupled state $|\Psi_{\gamma}\rangle \equiv b_{\gamma}^{\dagger}|0\rangle$ can be written as

$$b_{\gamma}^{\dagger} = z^{c} a_{\gamma}^{\dagger} + \sum_{dl} z_{dl}^{c} \left[a_{\delta}^{\dagger} Q_{\lambda}^{\dagger} \right]_{\gamma} + \sqrt{\frac{1}{2}} \sum_{dl'} z_{d2l'}^{c} \left[a_{\delta}^{\dagger} \left[Q_{2}^{\dagger} Q_{2}^{\dagger} \right]_{\lambda'} \right]_{\gamma}, \tag{10}$$

where $[\]_{7}$ means angular-momentum coupled to γ ; z, z_{dl} and $z_{d2l'}$ are, respectively, the qp, qp-phonon and qp-two-phonon amplitudes. In the actual computation only the phonons $l=2_1^+$, 3_1^- and 4_1^+ were considered and for the two-phonon term only the 2_1^+ phonon was considered, because $\omega_{2_1^+} \approx 1.2 \text{ MeV} \approx \frac{1}{2}\omega_{3_1^-} \approx \frac{1}{2}\omega_{4_1^+}$ in the even Sn isotopes.

Eq. (1), which implies a linear equation of motion for $b_1^{\dagger} \mid 0$ is derived by assuming that (i) Q^{\dagger} and Q obey boson commutation relations; (ii) the qp and phonon operators commute; (iii) | 0> is a phonon vacuum as well as a qp vacuum. These conditions are satisfied to a good degree of approximation when the physical state represented by a phonon operator does indeed arise from the collective motion of many (quasi) particles. The properties of the phonon will then be little affected by changes in any constituent single particle. The number of particles involved in the phonon $Q_{\tau}^{\dagger} | 0 \rangle$ is roughly equal to the strength of the $Q_1^{\dagger} \mid 0 \rangle \rightarrow 0$ transition, B(EI), in singleparticle, or Weisskopf units (W.u.). In the even Sn isotopes 10) B(E2) is about $10 \approx 15$ W.u. and B(E3) is about 25-30 W.u., suggesting that the number of particles involved in these phonons is indeed large. As the collectivity of the phonon decreases, effects of the neglected antisymmetrization terms (note that the coherent antisymmetrization terms are already included in the matrix element D_{vs1}) become more important, and the accuracy of the linear approximation worsens. In this context the problem of antisymmetrization in a two-level system has been solved by Bès et al. 22). In general, in the limiting case when the particle strengths are completely fragmented, the linear approximation breaks down and one must resort to the usual shell-model 460 H.-C. LEB

diagonalization procedure. Returning to the derivation of the equation of motion, we have, from the three assumptions stated above, the following commutators:

$$[H, a_{\gamma}^{\dagger}]|0\rangle = E_{c}a_{\gamma}^{\dagger}|0\rangle + \sum_{dl} D_{cdl}a_{dl,\gamma}^{\dagger}|0\rangle, \qquad (11a)$$

$$[H, a_{dl, \gamma}^{\dagger}]|0\rangle = (E_d + \omega_{l, \alpha} a_{dl, \gamma}^{\dagger}|0\rangle + D_{cdl} a_{\gamma}^{\dagger}|0\rangle + \sum_{al'} \delta_{l2} D_{da2} U(j_a 2j_c 2; j_d l') a_{a2l', \gamma}^{\dagger}|0\rangle, \qquad (11b)$$

$$[H, a_{d2l'}^{\dagger}, \gamma]|0\rangle = (E_d + 2\omega_2) a_{d2l', \gamma}^{\dagger}|0\rangle + 2\sum_{\sigma} D_{ed2} U(j_e 2j_\sigma 2; j_e l') a_{d2, \gamma}^{\dagger}|0\rangle, \qquad (11c)$$

where $a_{il, \gamma}^{\dagger} \equiv [a_{i}^{\dagger}Q_{i}^{\dagger}]_{\gamma}$, $a_{i2l', \gamma}^{\dagger} \equiv [a_{j}^{\dagger}[Q_{2}^{\dagger}Q_{2}^{\dagger}]_{k'}]_{\gamma}$ and $U(abcd; ef) = \sqrt{(2e+1)(2f+1)} \times W(abcd; ef)$ is the normalized Racah coefficient. From (11) and the equation of motion

$$[H, b_{\gamma}^{\dagger}]|0\rangle = \varepsilon_c b_{\gamma}^{\dagger}|0\rangle, \tag{12}$$

we obtain the secular equation for the amplitudes z, in block-matrix form

$$\begin{pmatrix} E_{c} - s_{c} & D_{cdl} & 0 \\ & \delta_{l2} \sqrt{2} D_{de2} \\ D_{cdl} & E_{d} + \omega_{l} - s_{c} & \times U(j_{a} 2 j_{c} 2; j_{d} l') \\ & \delta_{l2} \sqrt{2} D_{de2} \\ 0 & \times U(j_{a} 2 j_{c} 2; j_{d} l') & E_{a} + 2\omega_{2} - s_{c} \end{pmatrix} \begin{pmatrix} z^{c} \\ z^{c}_{dl} \\ z^{c}_{dl} \end{pmatrix} = 0.$$
 (13)

The residual interaction used in the calculations is derived from the nucleonnucleon interaction of Kahana, Lee and Scott ¹¹). Pairing correlations for the neutrons are taken into account for the neutrons ¹²), but not for the protons, since the Sn isotopes have a magic (50) proton number. Thus the low-lying states in the odd Sb (In) isotopes are described as proton particle-(hole) phonon coupled states. The neutron and proton sp energies, in ¹¹⁶Sn, for the twelve active orbits are given in table 1. The present calculation is in general not very sensitive to the s.p. energies of

TABLE 1
Single-particle energies for ¹¹⁶Sn

Orbit	Proton (MeV)	Neutron (MeV)	Orbit	Proton (MeV)	Neutron (MeV)
2p4	5.5	-5.5	384	1.3	0.7
1f ₄	-7.0	-5.0	2da	1.2	1.9
2p+	-5.2	-4.0	1hy	1.5	2.5
1gg	-4.9	-2.5	1hg	7.2	4.0
2d₄	0	0	2f ₂	6.8	5.0
1g ₂	0.2	0.5	li _#	9.5	7.5

the three highest orbits. However, the experimental level scheme of 115 In requires that the relative energies of the three proton orbits $2p_{\frac{1}{4}}$, $2p_{\frac{1}{4}}$ and $1g_{\frac{1}{4}}$ be more or less as given in table 1 and that the $1f_{\frac{1}{4}}$ orbit be ≈ 1 MeV more bound that the $1p_{\frac{1}{4}}$ orbit. The proton s.p. energy for orbit a in the isotope 4 Sn, where A is the atomic-mass number, is given by

$$E_a(A) = E_a(116) + \mu_a(A) - \mu_a(116),$$
 (14)

$$\mu_{a}(A) \equiv \sum_{c} \sqrt{\frac{2j_{c}+1}{2j_{a}+1}} v_{c}^{2}(A) F_{aacc0},$$
 (15)

where $v_c^2(A)$ is the occupation probability for the neutron orbit c in isotope ^ASn. The phonon states 2_1^+ , 3_1^- and 4_1^+ in the even Sn isotopes are described as two-qp vibrations. It has previously been shown ¹³) that experimental systematics of the level scheme and electromagnetic properties of the 2_1^+ and 3_1^- states in these nuclei are very satisfactorily accounted for by this description. Results obtained in refs. ^{12, 13}) are used for the present calculation, except for the excitation energies for the 2_1^+ and 3_1^- states, where the experimental values are used. In all cases spherical harmonic oscillator functions are used as wave functions for the s.p. orbitals. The oscillator frequency is taken to be proportional to $A^{-\frac{1}{2}}$ and is normalised to $\hbar\omega = 8.3$ MeV for ¹¹⁶Sn.

3. Results for the odd Sb isotopes

3.1. SYSTEMATICS OF THE LEVEL SCHEME OF LOW-LYING LEVELS

The theoretical (solid line) and experimental $^{14, 15}$) (dashed line) energies measured from the $\frac{1}{2}^+$ level of the $\frac{7}{2}^+$, $\frac{1}{2}^+$, $\frac{3}{2}^+$ and $\frac{11}{2}^-$ states are shown in fig. 1. As revealed by stripping reactions 15), these states are mainly single-particle states in the $2d_{\frac{1}{4}}$, $1g_{\frac{1}{4}}$, $3s_{\frac{1}{4}}$, $2d_{\frac{1}{4}}$ and $1h_{\frac{1}{4}}$ proton orbitals, respectively. The most prominent systematic in fig. 1 is the lowering of the $j = l - \frac{1}{2}$ (the $\frac{7}{2}^+$ and $\frac{3}{2}^+$) levels relative to the $j = l + \frac{1}{2}$ (the $\frac{4}{2}^+$, $\frac{1}{2}^+$ and $\frac{11}{2}^-$) levels, as the mass number increases. For example the ground state is switched from $\frac{5}{2}^+$ in 123 Sb to $\frac{7}{2}^+$ in 123 Sb. Theoretically this level crossing is almost entirely due to changes in the self-energy μ_a , defined in (15). This is shown in fig. 2, where $E(g_{\frac{1}{4}}) - E(d_{\frac{1}{4}})$ (solid line) and $s_{\frac{1}{4}1} - s_{\frac{1}{4}1}$ (dashed line) are plotted. Fig. 1 shows that the calculated energy shift between the $j = l + \frac{1}{2}$ and $j = l - \frac{1}{2}$ is only about 50% of the observed energy shift, thus suggesting that the spin dependence of the monopole F-matrix may be too weak.

3.2. THE AMPLITUDES x, x a AND x az

As a typical case, the amplitudes for 123 Sb are given in table 2. We note that $(z^c)^2 + \sum_{d} (z^c_{d2})^2 \approx 0.95$ for the two lowest $(\frac{7}{2}^+ \text{ and } \frac{5}{2}^+)$ states and ≈ 0.90 for the next two lowest $(\frac{1}{2}^+ \text{ and } \frac{3}{2}^+)$ states. This implies that the importance of the $a^{\dagger}_{d1,7} \mid 0 \rangle$ $(l \neq 2^+)$ and $a^{\dagger}_{d2l',7} \mid 0 \rangle$ components in these states is only marginal. These components become more important for the higher states. In particular the components

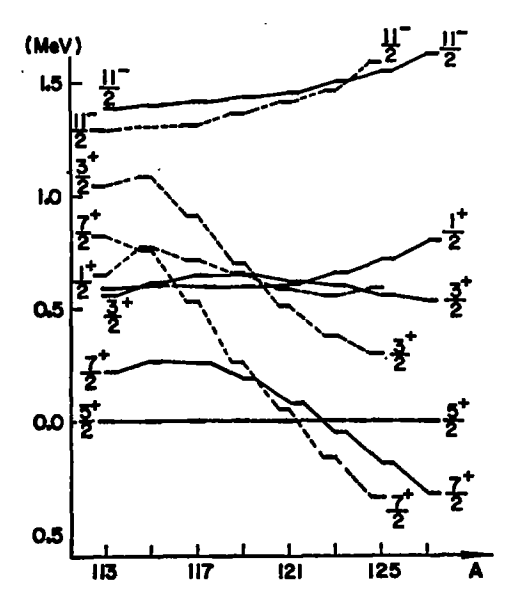


Fig. 1. Relative binding energies of low-lying levels in Sb isotopes. Dashed lines connect the experimental values and solid lines connect the computed values.

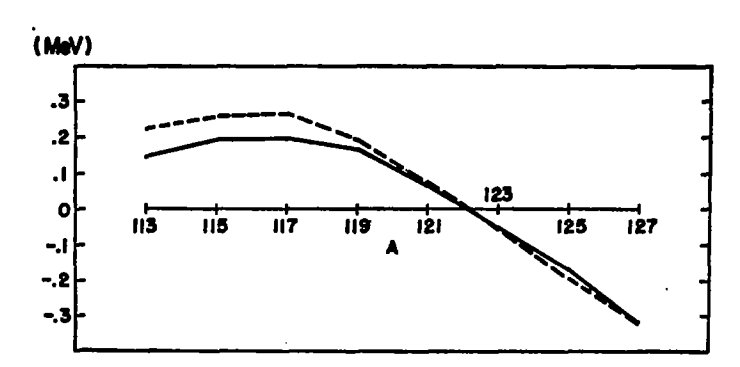


Fig. 2. Calculated relative binding energies of the $\frac{1}{4}$ ⁺ and $\frac{2}{4}$ ⁺ states. Dashed line: $\varepsilon_{\underline{q}}$ - $\varepsilon_{\underline{q}}$; solid line: $E(g_{\underline{q}})-E(d_{\underline{q}})$.

 $a_{d2l', \gamma}^{\dagger} | 0 \rangle$ of the $\frac{11}{2}^{+}$ and $\frac{9}{21}^{+}$ states contribute about 30% of the respective B(E2) strengths (see next section).

In table 3 a comparison is made between the theoretical s.p. amplitude z^c and spectroscopic amplitude \sqrt{S} , obtained from the stripping reaction ¹⁵) $^4\text{Sn}(^3\text{He}, d)^{A+1}\text{Sb}$ for the $\frac{5}{2}, \frac{7}{2}, \frac{1}{2}, \frac{1}{2}, \frac{3}{2}$ and $\frac{11}{2}$ states in the isotopes ¹¹³⁻¹²⁵Sb. In view of the fact that the uncertainty ¹⁵) in \sqrt{S} is of the order of 20 %, the agreement between theory and experiment is surprisingly good. In figs. 3 and 4 more detailed comparisons are made for all states with \sqrt{S} or $|z^c|$ greater than 0.3 in the two isotopes ¹¹⁹Sb and ¹²³Sb. The agreement between theory and data is slightly better

in ¹¹⁹Sb. The smaller calculated level spacings for the states at 1.5–2.0 MeV probably is an indication that the residual interaction may be somewhat too weak. In ¹²³Sb this small level spacing is also partly due to the fact that the calculated energy separations between the lowest $\frac{5}{2}$ and $\frac{7}{2}$ states, and the $\frac{1}{2}$ and $\frac{3}{2}$ states are too small. Un-

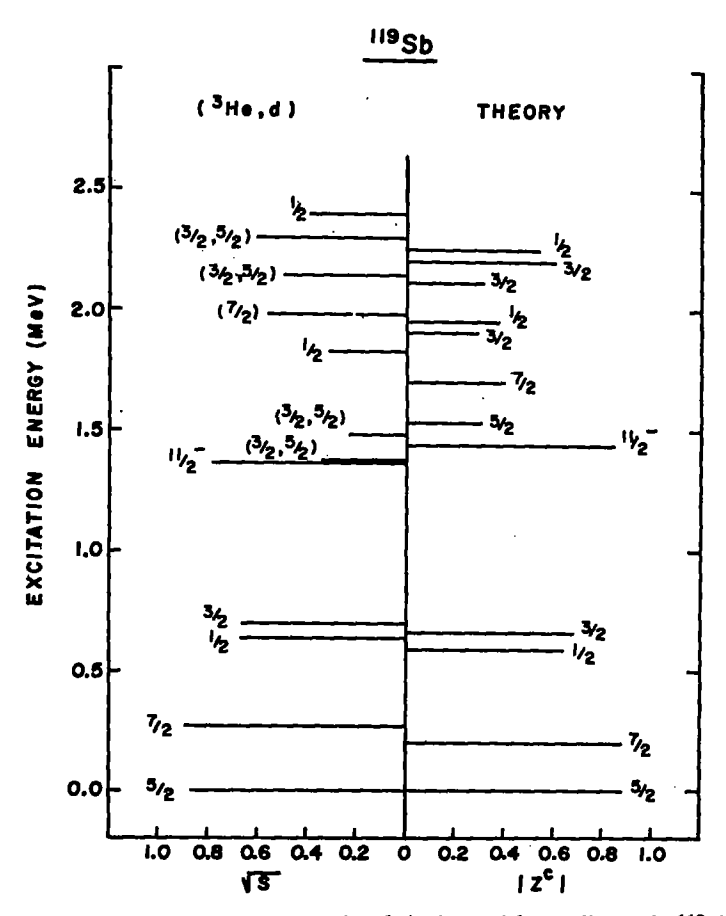


Fig. 3. Computed and empirical single-particle amplitudes in 119Sb.

doubtedly if we adjusted the input parameters, such as the single-particle and the phonon energies, in the calculation for each nucleus, a better agreement between theory and experimental data could be achieved.

3.3. E2 TRANSITION STRENGTHS

The reduced matrix element for the electric transition operator t_I between two

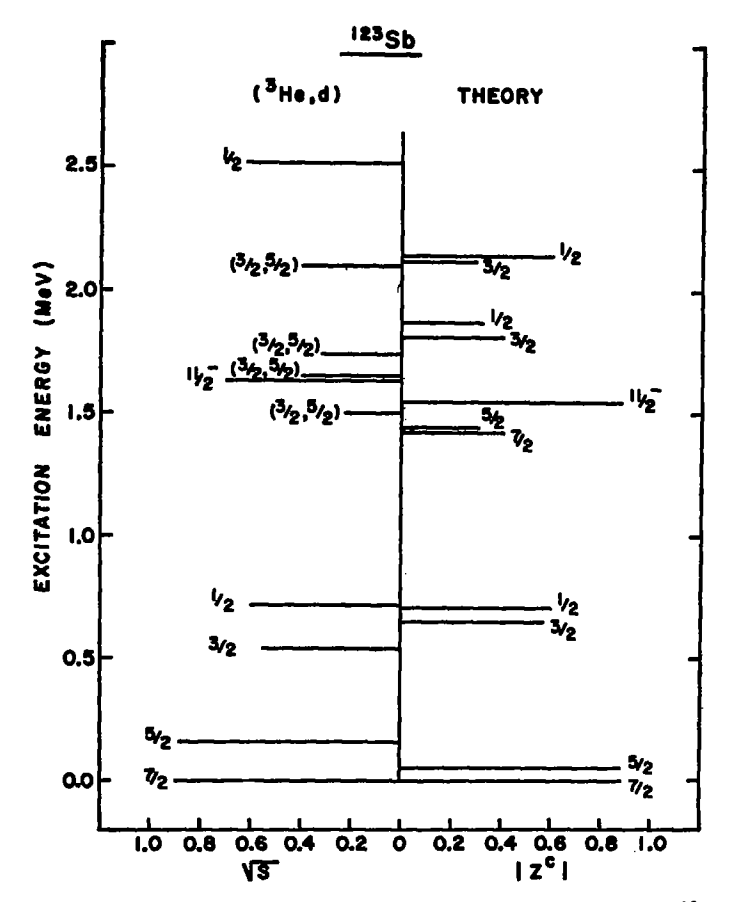


Fig. 4. Computed and empirical single-particle amplitudes in 123Sb.

particle-phonon coupled states is

$$\langle \psi_{c} || t_{J} || \psi_{a} \rangle = z^{c} z^{a} (u_{c} u_{a} - v_{c} v_{a} (\langle c || t_{J} || a \rangle + \sum_{dbll'} z_{bl}^{a} z_{bl'}^{a} [\delta_{ll'} (-)^{c+b+J+l} \partial W (dbca; Jl) (u_{d} u_{b} - v_{d} v_{b})$$

$$\times \langle d || t_{J} || b \rangle + \delta_{bd} (-)^{a-b+J-l} \partial W (ll'ca; Jd) \langle l || t_{J} || l' \rangle]$$

$$+ \frac{1}{f} \langle 0 || t_{J} || J \rangle \left\{ z_{aJ}^{c} z^{a} + (-)^{c-a+J} \frac{\partial}{\partial z} z^{c} z_{cJ}^{a} + \sqrt{2} \delta_{J2} \sum_{ll'} (-)^{a-d} \partial l' [z_{d2}^{c} z_{d2l'}^{a} W (2l'ca; Jd) + z_{d2l'}^{c} z_{d2}^{a} W (2l'ac; Jd)] \right\},$$
(16)

where $\langle c \mid \mid t_j \mid \mid a \rangle$ is the single-particle matrix element; $\langle 0 \mid \mid t_j \mid \mid J \rangle$ is the phonon transition matrix element; $a = \sqrt{2j_a + 1}$; and a has been used as a short-hand notation for j_a in the phase factors and the Racah coefficients. For the E2 transition $t_{2M} =$

TABLE 2
Wave functions for low-lying states in 123Sb

							•	•						
٦,	20		242		i i	Ze20°		ZE	Ze22 ^c			Zat	0.	
		(=p)	-in		-		*	Ŧ	+	-	+	-#	-	espe
+14	0.878	0.080	0.406	0	-0.140	0.075	0.003	-0.026	0	-0.052	0.036	0.086	-0.021	-0.022
+	0.898	0.321	-0.132	-0.148	0.088	0.029	0.001	-0.002	-0.046	0.022	0.053	-0.056	0	0.036
+14	-0.577	0.257	0.656	-0.154	-0.181	-0.105	0.065	0.250	-0.047	-0.037	0.099	0.092	0	•
+ 14	-0.595	0.698	0	0	0.244	-0.116	0.227	0	0	0.074	0	0.134	0	0
+	0	-0.154	0.881	0	0	0	-0.082	-0.226	0	0	0.020	0.365	0.030	-0.093
÷.	0	0	0.905	0	0	0	0	0.184	0	0	0.088	0.311	0	-0.173
+	0	0.903	0.150	0	0	0	0.119	-0.311	0	0	0.301	-0.017	-0.183	0.083
+	0.095	0.829	-0.349	0	-0.024	0	-0.208	0.113	0	-0.005	0.256	-0.226	-0.058	0.065
+	0.160	-0.039	0.918	-0.058	-0.084	-0.071	0.100	0.103	0.015	-0.111	0.054	0.274	0	-0.008
+ 5	-0.392	0.367	90.706	•,	0.061	0.225	-0.097	-0.210	0	-0.138	0.158	0.214	-0.014	0.012
J.		4		Ze2			Z43°			Ze20°	Le22		Ze24.	
						*		-‡0						
-1- -1-		0.859		0.389		0.276		-0.116		0.056	-0.060		0.083	
		-0.129		0.660		-0.520	_	0.375		0.176	-0.190		0.262	

	i +		2 +		1 +	1 +		‡ +		11 -	
A	theory *)	exp b)	theory	ехр	theory	ехр	theory	exp	theory	ехр	
113	0.87	0.84	0.86	0.97	0.60	0.71	0.68	0.76	0.81	0.63	
115	0.89	0.84	0.87	0.92	0.63	0.71	0.70	0.76	0.83		
117	0.89	0.84	0.88	0.90	0.65	0.77	0.70	0.65	0.84	0.72	
119	0.89	0.87	0.88	0.89	0.67	0.67	0.67	0.67	0.84	0.79	
121	0.89	0.85	0.88	0.84	0.62	0.55	0.62	0.52	0.85	0.79	
123	0.90	0.89	0.88	0.91	0.69	0.59	0.58	0.55	0.86	0.70	
125	0.90	0.90	0.89	0.86	0.57	0.50	0.52	0.57	0.87	0.87	

TABLE 3
Single-particle amplitudes in odd Sb isotopes

 $r^2Y_{2M}(\hat{r})$ and the transition strength is

$$B(E2; \psi_c \to \psi_b) = e^2 |\langle \psi_c || r^2 Y_2 || \psi_b \rangle|^2. \tag{17}$$

The static quadrupole moment for the state $|\psi_a\rangle$ is

$$Q_0(j_c) = e\sqrt{\frac{16}{5}}\pi\langle j_c j_c 20|j_c j_c\rangle\langle\psi_c||r^2 Y_2||\psi_c\rangle. \tag{18}$$

In the present calculation we ignore the term $\langle 2 \mid | t_2 \mid | 2 \rangle$ which is justified by noting that the Sn nuclei are basically spherical. Experimentally the quadrupole moment, which is proportional to $\langle 2 \mid | t_2 \mid | 2 \rangle$, of the Sn isotopes is consistent with zero ¹⁶). In the calculation ¹³) of the $B(E2; 0_1^+ \rightarrow 2_1^+)$ strengths in the Sn isotopes it was found that a charge enhancement of $\Delta e = 0.2e$ was needed for both valence protons and neutrons in order to bring the calculated values into agreement with the measured values. In the spirit of the unified theory the same charge enhancement should also be used, as a first order approximation, in the Sb isotopes. However, this value for Δe does not give a totally satisfactory result in comparing with data. In figs. 5 and 6 B(E2) values and the static quadrupole moments for the ground states in ¹²¹Sb and ¹²³Sb, respectively, are calculated as a function of Δe in the range $0.2e \leq \Delta e \leq 0.5e$. The $B(E2; 0_1^+ \rightarrow 2_1^+)$ as a function of Δe is calculated using the relation

$$\frac{B(\text{E2}; 0 \to 2; \Delta e)}{B(\text{E2}; 0 \to 2; \Delta e = 0)} = \left[1 + \frac{\Delta e}{e}(1+R)\right]^2,\tag{19}$$

where R=2.8 is the ratio of the quadrupole transition matrix elements for the neutron and proton densities ¹³) in the 2_1^+ state in Sn. In the present calculation we use the values ¹⁰) $B(E2; 0^+ \rightarrow 2_1^+; Ae = 0.2e) = 2040$ and $2000 e^2 \cdot \text{fm}^4$ for ¹²⁰Sn and ¹²²Sn, respectively. The experimental B(E2) values shown in figs. 5 and 6 are those compiled in the Nuclear Data Sheets ^{17, 18}). The original data were obtained from $(x, x'\gamma)$

^{*)} The coefficient x^c in eq. (10).

b) Spectroscopic amplitude \sqrt{S} , from ref. 15).

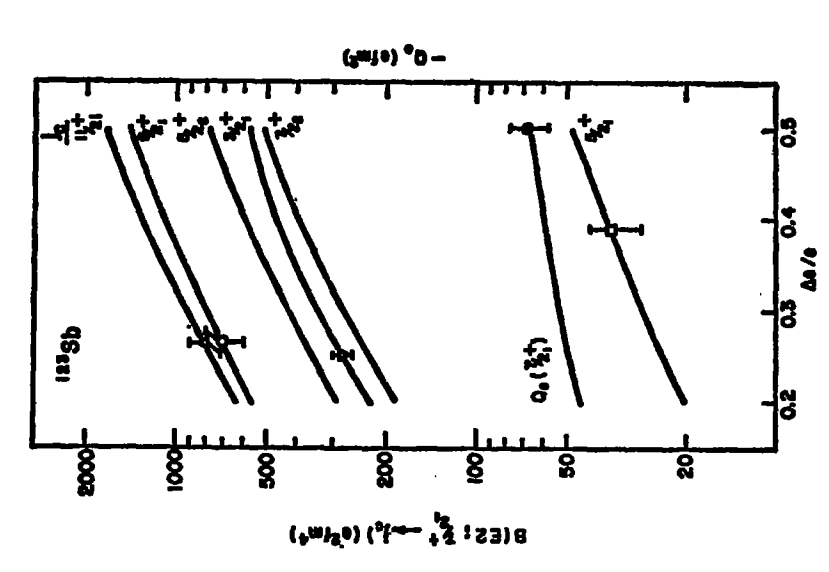


Fig. 6. Computed B(E2) values in 123Sb. Experimental data are from refs. 18, 19, 21).

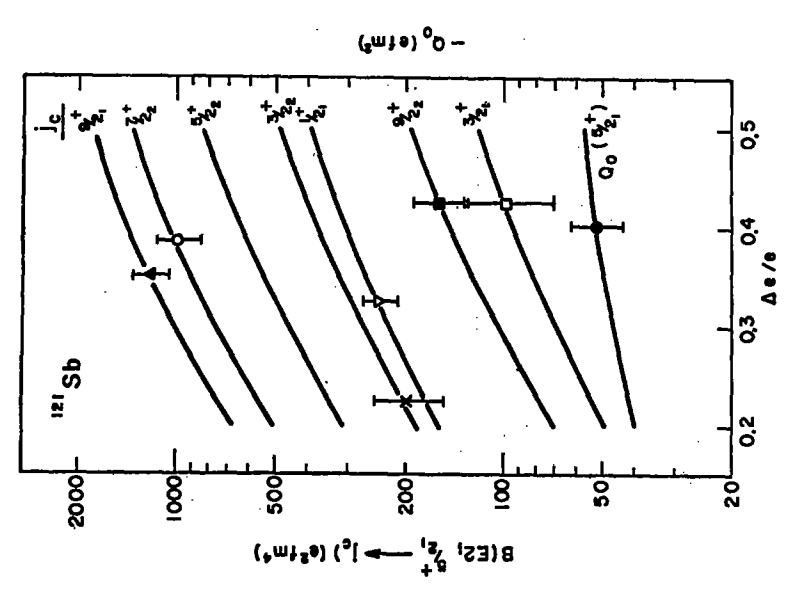


Fig. 5. Computed B(E2) values in ¹²¹Sb. Ae is the charge enhancement. Experimental points are from refs. ^{17, 19, 21}).

reactions. It is seen that although the best Δe is different for each transition the average value of $\Delta e=0.3e$ gives a very good description of the data. The theoretical fit to the twelve pieces of data produces a mean χ^2 of 1.56. The mean χ^2 increases to 4.81 when $\Delta e=0.20e$ is used. We have thus some evidence that the extra proton in Sb provides further polarization of the nucleus so as to make the effective charge for the valence particles in Sb slightly larger than that for the particles in Sn. The predicted (with $\Delta e=0.3e$) and observed Coulomb excitation schemes for the two nuclei are shown in figs. 7 and 8. The overall agreement between theory and experiment is very good.

There are very significant differences between the Coulomb excitation results of Barnes et al. ¹⁹) and those by Galperin et al. ²⁰), especially concerning the strongest transitions observed by the former group of investigators. Barnes et al. observed very large ($\approx 1000 \, e^2 \cdot \text{fm}^4$) strengths to the 1037 and 1147 keV levels in ¹²¹Sb and to the 1029 and 1087 keV levels in ¹²³Sb. The only transition of comparable strength observed by Galperin et al. in these nuclei is that to the 1032 keV level in ¹²³Sb. In this respect the present calculation supports the results of Barnes et al. and is in

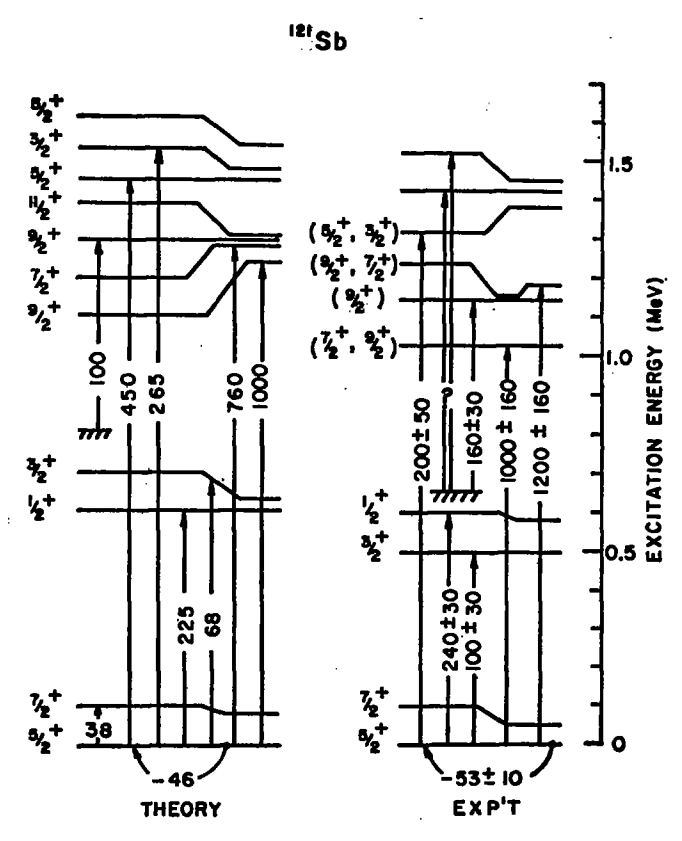


Fig. 7. Level scheme of ¹²¹Sb as seen in a (x, x'y) reaction. The B(E2) transition strengths are in units of $e^2 \cdot \text{fm}^2$. The ground-state quadrupole moment is in units of $e \cdot \text{fm}^2$.



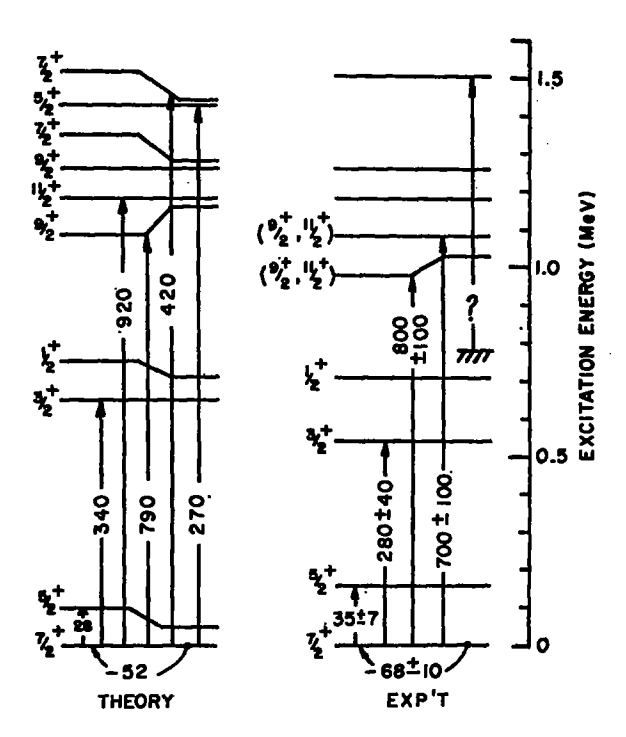


Fig. 8. Level scheme of ¹²³Sb. See caption of fig. 7.

rather serious disagreement with those of Galperin *et al.* Transitions with moderate strengths (200–400 $e^2 \cdot \text{fm}^4$) are predicted to go to the $\frac{1}{2}$ and $\frac{1}{2}$ levels at $\approx 1450 \text{ keV}$ in ¹²¹Sb and to the $\frac{1}{2}$ and $\frac{1}{2}$ levels at $\approx 1450 \text{ keV}$ in ¹²³Sb. Such transitions were observed at the 1423 and 1450 keV levels in ¹²¹Sb and at the 1502 keV level in ¹²³Sb but were not analysed ¹⁹).

The experimental quadrupole moments used in figs. 7 and 8 are those obtained from the method of optical spectroscopy 21). These values are in rather serious disagreement with those obtained using atomic beams 21), which are -29 and $-39e \cdot \text{fm}^2$, respectively, for ^{121}Sb and ^{123}Sb (the uncertainties in these results can be as large as 50%). Due to the large uncertainties in both sets of measurements the calculated values, which are very close to the respective means of the measured values favor neither set of experiments.

In figs. 7 and 8, the centroids of the B(E2) strengths are seen to be about 100 to 200 keV below the predicted location in the spectra. This may be due to some deficiency in the particle-phonon interaction. An overall increase in the interaction strength will not improve the situation, since it will depress the ground state more than the excited states. However, additional structure, or fluctuation in the D-matrix

elements would be present if the interactions which are non-collective in nature between the particle (proton) and the core (Sn) had been taken into account. In terms of particles and phonons such interactions are of higher order terms 22) than those considered in eq. (8). These non-collective residual interactions will modify the calculated spectra slightly but will not alter the distribution of B(E2) strengths in any significant way. The centroid of the B(E2) strength could also be lowered if we used quadrupole phonon energies which are, say, 150 keV lower than those observed in the corresponding Sn isotopes. Because core polarization affects the effective charge and the effective F-matrix in a similar manner, the fact that the phonon in Sb seems to be more collective ($B(E2; 0 \rightarrow 2; \Delta e = 0.3) \approx 1.48 B(E2; 0 \rightarrow 2; \Delta e = 0.2e)$) than the phonon in Sn strongly suggests that the effective quadrupole F-matrix in Sb may indeed be stronger and thus resulting in a lower energy for the 2^+ phonon.

4. Results for 115 In

In analogy to the Sb isotope, which was described as a proton coupled to Sn, here we describe In as a proton-hole coupled to Sn. We shall concentrate our study on ¹¹⁵In, which experimentally is the most extensively studied isotope.

The 116 Sn(d, 3 He) reactions 23) reveal that only the (hole) orbitals $g_{\frac{1}{2}}$, $p_{\frac{1}{2}}$ and $p_{\frac{1}{2}}$ have significant spectroscopic strength in 115 In. This information was in fact used to determine the relative single-particle energies of these orbitals shown in table 1. The calculated and measured single-particle strengths and excitation energies of the 2 +, 1 - and 3 - states are shown in table 4. The calculated single-particle strength for the 3 - state appears to be too large. Due to the fact that there is only one hole state with positive parity, the present model predicts a quintet of low excited positive-parity states (5 + to 13 +) of which the main component is $|g_{\frac{1}{2}}\otimes 2^{+}\rangle$, with smaller two-phonon components. Because of higher unperturbed energies and very weak couplings to the term mentioned above, the components $|p_{\frac{1}{2}}\otimes l\rangle$ and $|p_{\frac{1}{2}}\otimes l\rangle$, where $l=3^{-}$ or 4^{+} , can be totally ignored in calculating these positive-parity states. The calculated amplitudes for the low-lying states are shown in table 5 and the spectrum in fig. 9. Also shown in the figure are the predicted $B(E2\uparrow)$, with $\Delta e=0.3e$, and those extracted from Coulomb excitation 6 , 24). The most prominent feature in the observed

TABLE 4

Excitation energies and spectroscopic amplitudes of proton holes in ¹¹⁵In

j≅	Excitation	energy (MeV)		√S
	exp	theory	exp	theory
‡ 1 ⁺	0	0	0.86	0.88
1~	0.34	0.33	0.83	0.91
<u>*</u> ~	0.60	0.62	0.71	0.87
12+	1.47	1.58	0.42	0.49

transition scheme is the especially large strength going to the $\frac{11}{2}$ state. As was pointed out by Dietrich et al. ⁶) this is a consequence of the mixing of the two-phonon components into the dominantly one-phonon (plus proton-hole) states at ≈ 1.2 MeV. The present calculation confirms their findings. However, the coupling matrix element (derived from the realistic *F*-matrix) used here is less than two thirds the matrix element used by Dietrich et al. The major deficiency in the present calculation is that a B(E2) value of $890 \ e^2 \cdot \text{fm}^4$ is predicted for the transition to the $\frac{13}{2}$ state, as compared to the measured value e^{24} of $e^{24} \cdot e^{24}$. The calculation of Dietrich et al. yields a value of $e^{24} \cdot e^{24}$ and is in better agreement with experiment.

The dependence of the calculated B(E2) values on the charge enhancement is shown in fig. 10. As in the case for the Sb isotopes the value $\Delta e \approx 0.3e$ again gives the best agreement with experiment. Referring to our analysis in the last section, we see that the core polarization in Sn induced by an extra proton particle or proton hole is very nearly the same. Similarly, the predicted centroid of the B(E2) strength would be in better agreement with experiment if the quadrupole phonon energy in ¹¹⁵In were reduced by $\approx 150 \text{ keV}$ (see fig. 9). Unlike the Sb isotopes, measure-

Table 5
Wave functions for low-lying states in 115In

j _e	z e	Z ₄₂ °		2 ₄₂₀ c	Z ₄₂₂ c	$z_{424}^c \ (d=g_{\frac{a}{2}})$
1 1+	0.876	-0.434	-	0.066	-0.068	0.095
<u>\$</u> +	0	0.887		0	-0.436	-0.147
7 +	0	0.953		0	-0.020	-0.297
1 ₂ +	0.420	0.755	_	-0.236	0.243	-0.340
뀨+	0	0.845		0	0.332	-0.418
* +	0	0.895		0	-0.240	-0.380
j _c	Z ^c		Z42°		z ₁₄ 3°	
		$(d=) f_{\frac{4}{3}}$	P-	P÷		
<u>1</u> -	0.906	0.201	0.334	0		
1 -	0.868	0.085	-0.220	0.329	-0.287	

ments ²¹) of the quadrupole moment of ¹¹⁵In using atomic beam and using the method of optical spectroscopy yield almost identical results: $Q_0 \approx 83 e \cdot \text{fm}^2$. The predicted moment is smaller than, but not in disagreement with, the measured result.

So far we have not seen the 3^- phonon play any significant role in the low-lying states in Sb or in In. This is because the energy of this phonon, at ≈ 2 MeV, is comparatively high and the particle-phonon interaction (≈ 0.7 MeV) is too weak for

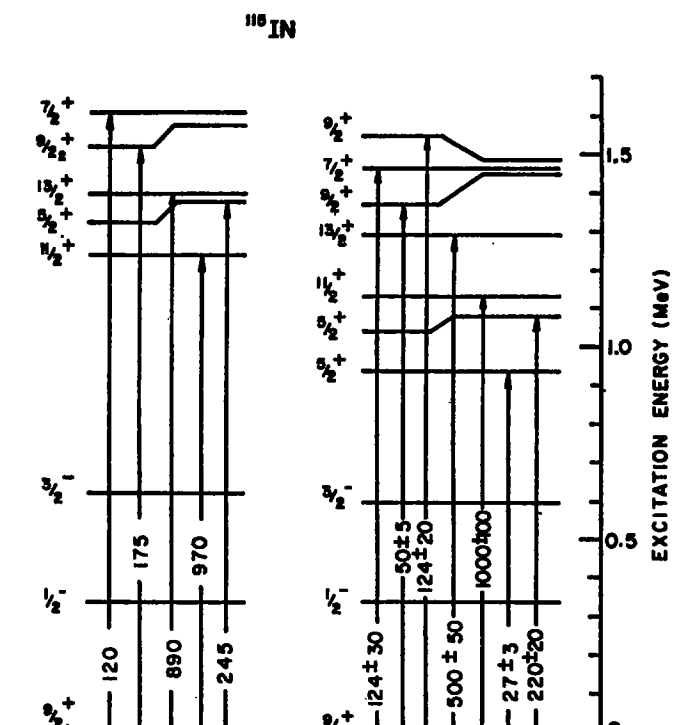


Fig. 9. Level scheme of 115 In. See caption of fig. 7.

EXP'T

its presence to be felt in the ≈ 1 MeV region. An exception may be found in the $\frac{3}{4}$ state at 600 keV.

THEORY

A B(E3) strength of $1.2 \times 10^4 \ e^3 \cdot \mathrm{fm}^6$ is calculated for the transition from the ground state to the 600 keV state. Since the predicted spectroscopic factor for the $\frac{3}{2}^-$ state is rather larger than the experimentally extracted value, which implies that the amplitude of the $(g_{\frac{1}{2}} \otimes 3^-)$ component in this state may be larger than we have calculated, the B(E3) strength given above should be taken as a lower limit. This strength could be measured, for example, in an (e, e') experiment.

There are several states below ≈ 1 MeV excitation that have been observed experimentally but not accounted for in the present model. The 828 $(\frac{1}{2}^+)$, 864 $(\frac{1}{2}^+)$, 934 $(\frac{7}{2}^+)$ and 941 $(\frac{5}{2}^+)$ keV levels have all been observed in the stripping $^{114}\text{Cd}(^3\text{He}, \text{d})$ reaction 25) but only the 934 keV state has a significant single-particle strength. These states, with the exception of the 934 keV level, which is very weakly populated, have not been observed in the pick-up $^{116}\text{Sn}(\text{d}, ^3\text{He})$ reaction. Among these states the only one that is observed in the (d, d') reaction 6) is the $\frac{5}{2}^+$ states at 941 keV, which presumably obtains its moderate E2 strength by mixing with

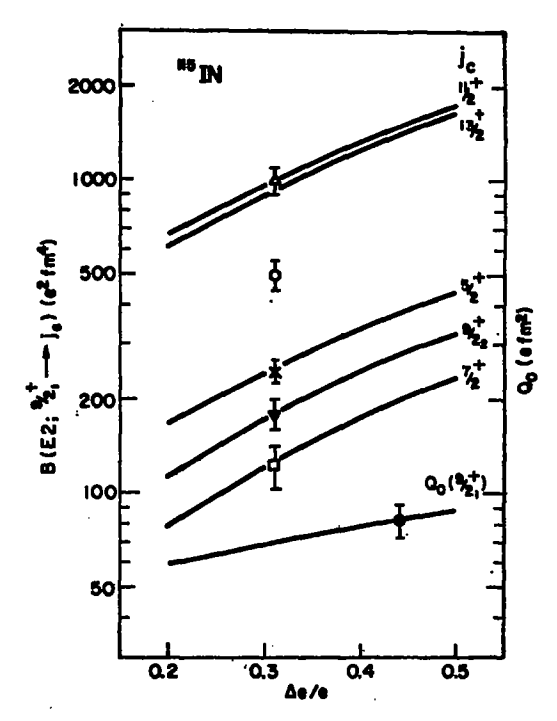


Fig. 10. Computed B(E2) values in 115 In. Experimental data are from refs. 6.21,24).

the $\frac{1}{2}$ state at 1078 keV. These four states thus have a structure which is more complex than can be described by the present model. In the pick-up reaction an l=3 state at 1040 keV is weakly populated. Presumably this is a small fragment of the $f_{\frac{1}{4}}$ orbital, which in our calculation is centered at ≈ 2 MeV excitation.

5. Summary

We have shown that in a unified theory the vibrational excitations in the Sn isotopes and the coupling of the extra proton particle (in Sb) and proton hole in (In) to these vibrations can be satisfactorily described by one and the same residual interaction. For the Sb and In isotopes quantitative agreement between theory and measured data is obtained even though no fine adjustments of parameters were attempted in order to achieve a "best fit". However, it is shown that agreement between calculated and measured B(E2) values is improved significantly when the charge enhancement, $\Delta e = 0.3e$, for the valence particles in Sb and In, is allowed to be slightly larger than that in Sn, where $\Delta e = 0.2e$. This implies an $\approx 50 \%$ increase of the $B(E2; 0_1^+ \rightarrow 2_1^+)$ value in the Sb or In isotopes over that in the Sn isotopes. Similarly the theoretical centroids of the B(E2) strengths from the ground states in Sb and In would agree better with the observed centroid if the quadrupole phonon

energies in these isotopes were allowed to be reduced by ≈ 150 keV compared to their unperturbed positions of ≈ 1.2 MeV in Sn. Although not easy to calculate, both of these effects can be understood as core polarizations induced by the extra proton particle or hole in Sb or In. Indeed, in the Te and Cd isotopes, corresponding to the Sn isotope plus two proton particles and holes, respectively, the $B(E2; 0_1^+ \rightarrow 2_1^+)$ values are 2 to 3 times larger than, and the quadrupole phonon energies about half the corresponding values in Sn [ref. 26)].

Because of the relatively high excitation energy of the octopole vibration and the lack of low-lying single-particle orbitals with negative parity in Sb, the octupole vibration plays essentially no role in the low-energy spectroscopy in Sb. In ¹¹⁵In, the $\frac{3}{2}$ state at 600 keV is predicted to have a non-negligible $(g_{\frac{3}{2}}\otimes 3^{-})$ component with a predicted $B(E3; \frac{9}{2}^{+} \rightarrow \frac{3}{2}^{-})$ strength of $\geq 1.3 \times 10^{4} \ e^{2} \cdot \text{fm}^{6}$. This, however, awaits experimental confirmation.

References

- 1) L. L. Foldy and F. J. Milford, Phys. Rev. 80 (1950) 751
- 2) A. Bohr and B. R. Mottelson, Mat. Fys. Medd. Dan. Vid. Selsk. 27, no. 16 (1953)
- 3) B. Castel, K. W. Stewart and M. Harvey, Can. J. Phys. 47 (1970) 1490
- 4) I. Hamamoto, Nucl. Phys. A126 (1969) 545; A141 (1970) 1
- 5) G. Vanden Berghe and K. Heyde, Phys. Lett. 32B (1970) 173
- 6) F. S. Dietrich, B. Herskind, R. A. Naumann and R. G. Stokstad, Nucl. Phys. A155 (1970) 209
- 7) G. E. Brown, Unified theory of nuclear models, 2nd ed. (North-Holland, Amsterdam, 1967)
- N. N. Bogoljubov, Nuovo Cim. 7 (1958);
 J. G. Valatin, ibid. 7 (1958) 843
- 9) M. Baranger, Phys. Rev. 120 (1960) 957
- 10) P. H. Stelson, F. K. McGowan, R. L. Robinson and W. T. Milner, Phys. Rev. C2 (1970) 2015
- 11) S. Kahana, H. C. Lee and C. K. Scott, Phys. Rev. 180 (1969) 956
- 12) H. C. Lee and K. Hara, Phys. Rev. C3 (1971) 325
- 13) H. C. Lee, Nucl. Phys. A255 (1975) 86
- 14) J. H. E. Mattauch, W. Thiele and A. H. Wapstra, Nucl. Phys. 67 (1965) 1
- 15) M. Cojeaud, S. Harer and Y. Cassagnon, Nucl. Phys. A117 (1968) 449
- 16) A. Christy and O. Häusser, Nucl. Data Tables 11 (1973) 281
- 17) D. J. Horen, Nucl. Data Sheets B6 (1971) 75
- 18) R. L. Auble, Nucl. Data Sheets B7 (1972) 363
- 19) P. D. Barnes, C. Ellegaard, B. Herskind and M. C. Joshi, Phys. Lett. 23 (1966) 266
- L. N. Galperin, A. Z. Ilyasov, I. K. Lemberg and G. A. Firsonv, Sov. J. Nucl. Phys. 9 (1969) 133
- 21) G. H. Fuller and V. W. Cohen, Nucl. Data Tables A5 (1969) 433
- 22) D. R. Bès, G. G. Dussel, R. A. Broglia, R. Liotta and B. R. Mottelson, Phys. Lett. 52B (1974) 253
- W. H. A. Hesselink, B. R. Kooistra, L. W. Put, R. H. Siemssen and S. Y. van der Werf, Nucl. Phys. A225 (1974) 229
- 24) S. Raman and H. J. Kim, Nucl. Data Sheets 16 (1975) 195
- 25) E. Thuriere, Thesis, University of Paris (1970), quoted in ref. 24)
- 26) C. M. Lederer, J. M. Hollander and I. Perlman, Table of isotopes, 6th ed. (Wiley, NY, 1968)